Simulation studies of energy transfer to heavy ions by strong current-driven instabilities

Mieko Toida, Akihiro Sugishima, and Yukiharu Ohsawa
Department of Physics, Nagoya University, Nagoya 464-8602, Japan

(Received 17 October 2001; accepted 7 March 2002)

Energy transfer from electrons to heavy ions via the nonlinear evolution of instabilities driven by strong currents is studied by means of a two-dimensional, electrostatic, particle simulation code with full ion and electron dynamics. Electrons are assumed to drift along a uniform magnetic field with an initial speed larger than the electron thermal speed in a plasma consisting of hydrogen (H) and helium (He) ions and electrons. Simulations then show that, because of the electron trapping by the Buneman waves which grow at first, the shape of the electron velocity distribution function $f_e(v_\parallel)$ is drastically changed and is significantly broadened. Then, H cyclotron waves, which are marginal in the initial state, are destabilized and grow to large amplitudes. Their frequencies are higher than those predicted by the linear theory. Although He ions do not gain energies from the Buneman waves, they are heated by H cyclotron waves. As a result of the instabilities, $f_e(v_\parallel)$ has a plateau region with its width much greater than the initial thermal speed. © *2002 American Institute of Physics.* [DOI: 10.1063/1.1474423]

I. INTRODUCTION

High-energy heavy ions are often observed in space plasmas. For instance, in some solar flares, the abundance of high-energy ^{3}He ions and heavier ions such as Fe, Si, Mg, etc., are enhanced.[1–7] In the Earth's ionosphere, oxygen ions, O^+ are often heated perpendicular to the geomagnetic field.[8–11] Motivated by these observations, energy transfer from electrons to heavy ions through current-driven instabilities has been extensively studied.[12–18] However, those studies are mainly based on linear theories and have not succeeded in quantitatively explaining the observations. We must study, in a self-consistent manner, both the nonlinear evolution of instabilities and energy transport among different particle species. Then, we need to make a nonlinear theory and discuss the energy transport in the solar corona or in the Earth's ionosphere.

Recently, with particle simulations, current-driven instabilities in a plasma consisting of hydrogen (H) and helium (He) ions and electrons have been studied.[19] In that study, electrons were assumed to drift along a uniform magnetic field with an initial speed equal to the electron thermal speed, $v_{d0}=v_{Te}$. The linear theory based on the initial conditions predicting that ion acoustic waves would be the most unstable and that the second harmonic H cyclotron waves were only marginal.[22] However, the simulations demonstrated that the ion acoustic waves quickly saturate to small amplitudes and that the second harmonic waves eventually become dominant owing to the change in the electron parallel velocity distribution function $f_e(v_\parallel)$. The second harmonic waves were observed to heat He ions more than H ions. These simulation results indicate that the linear theory cannot predict which waves become dominant and which particle species are heated.

In Ref. 20, then, a nonlinear theory predicting dominant modes was developed. Theoretical estimates of energy gains of ions from the waves were also presented. The theory shows that, as a result of the wave development through the change of $f_e(v_\parallel)$, the energy transfer to heavy ions can be enhanced much more than the linear theory predicts.

Those studies were on weak currents, $v_{d0}=v_{Te}$. In space plasmas, stronger currents such as $v_{d0}\gg v_{Te}$ would be important in heavy ion heating. Some observations showed that, in the Earth's ionosphere, strong currents cause energy transfer to heavy ions O^+.[10,11] However, the linear theory cannot explain these observations; heavy ions cannot respond to Buneman waves excited by strong currents. Also, it was observed that the electrons with a velocity distribution function much wider than the usual thermal speed are correlated with the O^+ heating.[10,11] This has been an unresolved problem.

In this paper, we study the instabilities driven by strong current in a plasma consisting of H, He, and electrons, by means of a two-dimensional electrostatic particle code with full ion and electron dynamics. It is demonstrated that, as a result of the nonlinear evolution, He ions are heated perpendicular to the magnetic field, and the electron velocity distribution function $f_e(v_\parallel)$ is drastically broadened. (This simulation result qualitatively agrees with the observations.) The heating of He ions is by the H cyclotron waves which are only marginal in the initial state and are destabilized via drastic change of $f_e(v_\parallel)$ due to Buneman waves.

We assume that the initial electron velocity distribution is a shifted Maxwellian, although this distribution could hardly be formed in the space. However, we would like to say that the shape of the initial distribution is not essential in the process shown by the simulation. Even if we start with the different distribution function, the nonlinear development of waves through self-consistent change in $f_e(v_\parallel)$ and the heavy ion heating would occur. Therefore, the present simulation result would be an important clue to the problem of

 © 2002 American Institute of Physics

Downloaded 27 Oct 2006 to 133.6.32.11. Redistribution subject to AIP license or copyright, see http://pop.aip.org/pop/copyright.jsp

energy transfer to heavy ions via instabilities driven by strong currents in space plasmas.

In Sec. II, we describe a linear theory of Buneman waves and H cyclotron waves. In Sec. III, we present results of the simulation where the initial electron drift speed is taken to be $v_{d0}=3v_{Te}$. It will be shown that the Buneman waves have significant nonlinear effects. The Buneman waves grow firstly and produce electric potential larger than the electron temperature. Because some electrons are trapped by the potential, $f_e(v_\parallel)$ is drastically deformed and is broadened much more than in the weak current case with $v_{d0}=v_{Te}$.[19] The parallel electron temperature becomes about six times as high as the initial value. The change in $f_e(v_\parallel)$ destabilizes H cyclotron waves, which are only marginal in the initial state. Their frequencies are observed to be higher than the theoretical values based on the linear theory. We note that the wave frequencies in the simulations with small currents were in good agreement with the linear theory.[19] The frequency increase is due to the rise of the electron temperature. Because of the Buneman waves and H cyclotron waves, $f_e(v_\parallel)$ finally has a plateau region, the width of which is much larger than the initial thermal speed.

The strong currents cause energy transfer to H and He ions with different mechanisms. The Buneman waves rapidly accelerate H ions, because some H ions are reflected by the electric potential. On the other hand, He ions are gradually heated by H cyclotron waves. The frequency increase of H cyclotron waves plays an important role in the heating of He ions. A summary of our work will be given in Sec. IV.

II. LINEAR THEORY

Before presenting simulation results, we will describe some properties of Buneman waves and H cyclotron waves based on their linear dispersion relations.

We consider a plasma consisting of H, He, and electrons. We assume that the electrons have temperature anisotropy and drift along the uniform magnetic field; the initial electron distribution function is written as

$$F_{e0}(v_\parallel,v_\perp)=\frac{1}{(2\pi)^{3/2}v_{Te\parallel}^2 v_{Te\perp}}\exp\left(-\frac{v_\perp^2}{2v_{Te\perp}^2}\right)\times\exp\left(-\frac{(v_\parallel-v_{d0})^2}{2v_{Te\parallel}^2}\right). \tag{2.1}$$

Here, the subscripts $\parallel$ and $\perp$ denote quantities parallel and perpendicular to the magnetic field, respectively. For ions, isotropic Maxwellian velocity distribution functions are assumed,

$$F_{i0}(v_\parallel,v_\perp)=\frac{1}{(2\pi v_{Ti})^{3/2}}\exp\left(-\frac{v_\perp^2+v_\parallel^2}{2v_{Ti}^2}\right). \tag{2.2}$$

The subscript i refers to denotes H or He.

We consider a low-β plasma where electrostatic waves are likely excited.[13] We neglect the effects of the electromagnetic waves. The linear dispersion relations of electrostatic waves are obtained from the set of Vlasov equation and Gauss's law as

$$1+\sum_{i=H,He}\frac{\omega_{pi}^2}{k^2v_{Ti}^2}\times\left[1+\sum_{n=-\infty}^{\infty}\frac{\omega}{\sqrt{2}k_\parallel v_{Ti}}Z\left(\frac{\omega-n\Omega_i}{\sqrt{2}k_\parallel v_{Ti}}\right)\Gamma_n(\mu_i)\right]+\frac{\omega_{pe}^2}{k^2v_{Te\parallel}^2}\left[1+\sum_{n=-\infty}^{\infty}\left(\frac{v_{Te\parallel}^2}{v_{Te\perp}^2}\frac{n\Omega_e}{\sqrt{2}k_\parallel v_{Te\parallel}}+\frac{\omega-k_\parallel v_{d0}-n\Omega_e}{\sqrt{2}k_\parallel v_{Te\parallel}}\right)\Gamma_n(\mu_e)Z\left(\frac{\omega-k_\parallel v_{d0}-n\Omega_e}{\sqrt{2}k_\parallel v_{Te}}\right)\right]=0, \tag{2.3}$$

where k is the wave number; ω is the complex frequency; Ω_j is the cyclotron frequency ($\Omega_e<0$) with $j=$H, He, or e; ω_{pj} is the plasma frequency; Z is the plasma dispersion function defined as[23]

$$Z(\xi)=\frac{1}{\sqrt{\pi}}\int_{-\infty}^{\infty}dx\,\frac{\exp(-x^2)}{x-\xi}. \tag{2.4}$$

Also, J_n is the Bessel function of the nth order, and $\Gamma_n(\mu_j)$ is $\Gamma_n(\mu_j)=I_n(\mu_j)\exp(-\mu_j)$, where I_n is the modified Bessel function of the nth order. The quantity μ_j is defined as $\mu_j=k_\perp^2\rho_j^2$ with ρ_j being the gyro-radius, $\rho_j=v_{Tj\perp}/|\Omega_j|$.

A. Buneman instability

When the electron drift velocity v_{d0} is much larger than the parallel thermal velocity $v_{Te\parallel}$, the Buneman waves are unstable.[21] Their dispersion relations can be found under the assumptions that

$$|\omega-n\Omega_e-k_\parallel v_{d0}|/(k_\parallel v_{Te\parallel})\gg 1,$$
$$|\omega-n\Omega_i|/(k_\parallel v_{Ti})\gg 1,\quad \mu_i\ll 1,\quad \mu_e\ll 1. \tag{2.5}$$

Retaining the lowest-order ($n=0$) terms of electrons and ions in Eq. (2.3), we obtain the frequencies ω_r, growth rates γ and the parallel wave numbers $k_\parallel$ of the fastest growing Buneman waves as

$$\omega_r=\frac{1}{2}\left(\frac{\Sigma_i\omega_{pi}^2}{2\omega_{pe}^2}\right)^{1/3}\frac{\omega_{pe}\cos\theta}{[1+\Sigma_i(\omega_{pi}/\Omega_i)^2\sin^2\theta]^{1/2}}, \tag{2.6}$$

$$\gamma=\sqrt{3}\omega_r, \tag{2.7}$$

$$k_\parallel v_{d0}=\omega_{pe}\cos\theta/\left[1+\sum_i(\omega_{pi}/\Omega_i)^2\sin^2\theta\right]^{1/2}. \tag{2.8}$$

Here, θ is the angle between the wave vector and the magnetic field: $\cos\theta=k_\parallel/k$ and $\sin\theta=k_\perp/k$. The wave propagating along the magnetic field, $\theta=0$, has the greatest growth rate. The phase velocity of the Buneman wave $\omega/k_\parallel$ is much smaller than the electron drift velocity v_{d0}. When the electron velocity distribution is a shifted Maxwellian with v_{d0} much larger than v_{Te}, there are few electrons whose velocities are equal to $\omega/k_\parallel$. The phase velocity is also much larger than v_{Ti}

$$\frac{\omega}{k_\parallel v_{Ti}}\simeq\left(\frac{m_i}{m_e}\right)^{1/6}\frac{v_{d0}}{v_{Te}}\gg 1. \tag{2.9}$$

Downloaded 27 Oct 2006 to 133.6.32.11. Redistribution subject to AIP license or copyright, see http://pop.aip.org/pop/copyright.jsp

Hence, the energy transfer to ions through Landau resonance with the Buneman wave is negligible.

B. H cyclotron waves

For H cyclotron waves, we assume that

$$|\omega - k_\parallel v_{d0}|/(k_\parallel v_{Te\parallel}) \ll 1, \quad |\omega - n\Omega_i|/(k_\parallel v_{Ti}) \gg 1,$$
$$|\Omega_e|/(k_\parallel v_{Te}) \gg 1, \quad \mu_e \ll 1. \tag{2.10}$$

Then, retaining the lowest order ($n=0$) term of electrons, the $n=0$ and nth order terms of H ions, and the $n=0$ and $2n$th order terms of He ions in Eq. (2.3), we obtain the frequency and growth rates of nth harmonic H cyclotron waves as[24,25]

$$\omega_r = n\Omega_H + n\Omega_H \left[\Gamma_n(\mu_H) + \frac{v_{TH}^2 \omega_{pHe}^2}{v_{THe}^2 \omega_{pHe}^2} \Gamma_{2n}(\mu_{He}) \right] \times \left\{ \frac{v_{TH}^2 \omega_{pe}^2}{v_{Te\parallel}^2 \omega_{pH}^2} \left[1 - \frac{(n\Omega_H - k_\parallel v_{d0})^2}{2k_\parallel^2 v_{Te}^2} \right] + 1 - \Gamma_0(\mu_H) + \frac{v_{TH}^2 \omega_{pHe}^2}{v_{THe}^2 \omega_{pH}^2} [1 - \Gamma_0(\mu_{He})] \right\}^{-1}, \tag{2.11}$$

$$\gamma_n \simeq \sqrt{\frac{\pi}{2}} \frac{(\omega_r - n\Omega_H)^2}{n\Omega_H \Gamma_n(\mu_H)} \frac{\lambda_{DH}^2}{\lambda_{De}^2} \frac{(v_{d0} - v_c)}{v_{Te\parallel}}. \tag{2.12}$$

Here, v_c is the critical speed for the instabilities and is defined as

$$v_c = \frac{\omega_r}{k_\parallel} \left[1 + \frac{\omega_{pH}^2 v_{Te\parallel}^3}{\omega_{pe}^2 v_{TH}^3} \Gamma_n(\mu_H) \exp\left(- \frac{(\omega_r - n\Omega_H)^2}{2k_\parallel^2 v_{TH}^2} \right) + \frac{\omega_{pHe}^2 v_{Te\parallel}^3}{\omega_{pe}^2 v_{THe}^3} \Gamma_{2n}(\mu_{He}) \exp\left(- \frac{(\omega_r - 2n\Omega_{He})^2}{2k_\parallel^2 v_{THe}^2} \right) \right]. \tag{2.13}$$

When $v_{d0} > v_c$, the waves are unstable. The growth rates of H cyclotron waves are much smaller than those of the Buneman waves.

According to Eq. (2.11), the frequencies of H cyclotron waves depend on the electron parallel temperature, but do not on the perpendicular temperature. For the waves with $\mu_i \ll 1$, the frequencies can be written as

$$\omega_r \simeq n\Omega_H \left[1 + \Gamma_n(\mu_H) \frac{v_{Te\parallel}^2 \omega_{pH}^2}{v_{TH}^2 \omega_{pe}^2} \right]. \tag{2.14}$$

This equation shows that ω_r increases with $v_{Te\parallel}$.

Suppose that the electron distribution function $F_{e0}(v_\parallel, v_\perp)$ can be written as

$$F_{e0}(v_\parallel, v_\perp) = \frac{1}{(2\pi)^{3/2} v_{Te\perp}^2 v_{Te\parallel}} \exp\left(- \frac{v_\perp^2}{2v_{Te\perp}^2} \right) g(v_\parallel), \tag{2.15}$$

then the growth rates of H cyclotron waves are given by[20]

$$\gamma_n \simeq \alpha_n \left[\frac{\omega_{pe}^2}{v_{Te\parallel}} \frac{\partial g(v_\parallel)}{\partial v_\parallel} \bigg|_{v_\parallel = \omega_r/k_\parallel} - \sum_{i=H,He} \sum_{n'} \frac{\omega_{pi}^2}{v_{Ti}^3} \frac{\omega_r \Gamma_n'(\mu_i)}{k_\parallel} \times \exp\left(- \frac{(\omega_r - n'\Omega_i)^2}{2k_\parallel^2 v_{Ti}^2} \right) \right], \tag{2.16}$$

with α_n,

$$\alpha_n = \left[\frac{1}{\lambda_{DH}^2} \sum_{n'} \frac{n'\Omega_H \Gamma_{n'}(\mu_H)}{(\omega_r - n'\Omega_H)^2} + \frac{1}{\lambda_{DHe}^2} \sum_{n'} \frac{n'\Omega_{He} \Gamma_{n'}(\mu_{He})}{(\omega_r - n'\Omega_{He})^2} \right]^{-1}. \tag{2.17}$$

Here, in order to obtain more accurate growth rates than Eq. (2.12), we have retained all terms for H and He ions.

The second term in Eq. (2.16) represents the damping due to the cyclotron resonance of ions. Therefore, using this term, we can estimate the energy transfer to ions from a nth harmonic H cyclotron wave as

$$\frac{dK_i}{dt} = n_i \beta_i |E_k|^2, \tag{2.18}$$

where β_i is defined as

$$\beta_i = \frac{\epsilon_k \alpha_n \omega_r}{2k_\parallel} \frac{q_i^2}{m_i v_{Ti}^3} \sum_{n'} \Gamma_{n'}(\mu) \exp\left(- \frac{(n'\Omega_i - \omega)^2}{2k_\parallel^2 v_{Ti}^2} \right). \tag{2.19}$$

Here q_i is ion charge, m_i is the ion mass, and ϵ_k is given by[20]

$$\epsilon_k = 1 + \frac{\omega_{pe}^2}{k^2 v_{Te\parallel}^2} + \sum_{i=H,He} \sum_m \frac{\Omega_i^2 \Gamma_m(\mu_i)}{k^2 \lambda_{Di}^2 (\omega_r - m\Omega_i)^2}. \tag{2.20}$$

III. SIMULATION

To study the development of the Buneman waves and H cyclotron waves and associated energy transport, we have performed simulations using a two-dimensional (two space and three velocity components), electrostatic particle code with full ion and electron dynamics.[26,27] The system size is $L_x \times L_y = 256\Delta_g \times 1024\Delta_g$, where Δ_g is the grid spacing. We use periodic boundary conditions in both x and y directions. The code has three particle species; H, He, and electrons. Their total numbers are $N_H = 27, 787, 264$, $N_{He} = 2, 883, 584$, and $N_e = 33, 544, 432$. The mass ratios are $m_H/m_e = 100$ and $m_{He}/m_H = 4$; the charge ratios are $q_H/|q_e| = 1$ and $q_{He}/q_H = 2$; the electron cyclotron frequency is $|\Omega_e|/\omega_{pe} = 2.0$. The external magnetic field is in the y direction.

Initially, the electrons have a shifted Maxwell distribution, Eq. (2.1), with $v_{Te\parallel} = v_{Te\perp}$. In the following, we write the initial electron thermal speed as v_{Te}. The drift speed is taken to be $v_{d0} = 3v_{Te}$. The temperature ratios are $T_e/T_H = 5.0$ and $T_{He}/T_H = 1$. The ion gyro-radii are $\rho_H = \rho_{He} = 2.24\lambda_{De}$. The grid spacing is equal to the electron Debye length, $\Delta_g = \lambda_{De}$. The system covers the wave numbers $0 \leqslant k_\parallel \lambda_{De} \leqslant 3.1$ and $0 \leqslant k_\parallel \lambda_{De} \leqslant 3.1$ with the spacing $\Delta(k_\parallel \lambda_{De}) = 6.1 \times 10^{-4}$ and $\Delta(k_\perp \lambda_{De}) = 2.5 \times 10^{-3}$. We solve the initial value problem of this system. The time step is $\omega_{pe}\Delta t = 0.15$.

Downloaded 27 Oct 2006 to 133.6.32.11. Redistribution subject to AIP license or copyright, see http://pop.aip.org/pop/copyright.jsp

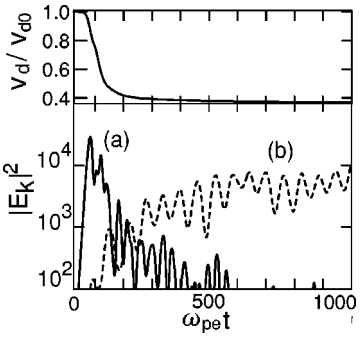

FIG. 1. Time variations of electron drift speed and $|E_k|^2$ of a Buneman wave and H cyclotron wave. The solid line (a) shows the Buneman wave with $(k_\parallel\lambda_{De}, k_\perp\lambda_{De})=(0.39,0)$. The dashed line (b) represents the H cyclotron wave with $(k_\parallel\lambda_{De}, k_\perp\lambda_{De})=(0.018,0.17)$. Here, $|E_k|^2$ is normalized to $m_e v_{Te}^2$.

According to the linear theory based on the initial conditions, the Buneman waves are unstable. The wave with $(k_\parallel\lambda_{De}, k_\perp\lambda_{De})=(0.39,0)$ has the greatest growth rate, $\gamma=0.089\omega_{pe}$, which is obtained from the numerical calculation of Eq. (2.3). Fundamental and second harmonic H cyclotron waves are also unstable. However, their growth rates, which are at most $\gamma\simeq 0.008\omega_{pe}$, are much smaller than those of the Buneman waves. Ion acoustic waves and He cyclotron waves are stable.

A. Wave evolution

In this subsection, we show the nonlinear evolution of Buneman waves and H cyclotron waves. It will be shown that Buneman waves quickly saturate, and H cyclotron waves are destabilized later and grow to large amplitudes, although they are marginal in the initial state. The observed frequencies of H cyclotron waves are higher than the theoretical values based on the linear theory.

Figure 1 shows time variations of the electron drift speed (parallel velocity averaged over all electrons) and amplitudes of two typical modes. Here, the drift speed is normalized to its initial value. The electric field energy $|E_k|^2$ is normalized to $m_e v_{Te}^2$. The solid line (a) in the lower panel represents the Buneman wave with the wave number $(k_\parallel\lambda_{De}, k_\perp\lambda_{De})=(0.39,0)$. The dashed line (b) shows the second harmonic H cyclotron wave with $(k_\parallel\lambda_{De}, k_\perp\lambda_{De})=(0.018,0.17)$. We will refer to these modes as mode (a) and (b), respectively. The theoretical initial growth rate γ and frequency ω of mode (a) are $\gamma=0.089\omega_{pe}$ and $\omega=0.082\omega_{pe}$. On the other hand, mode (b) is initially almost stable; the theoretical frequency is $\omega\simeq 2.02\Omega_H$.

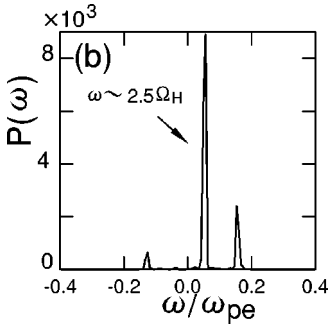

FIG. 3. Frequency spectrum for mode (b). Note that $\Omega_H=0.020\omega_{pe}$.

In the early stage, the electron drift speed quickly decays with time, and mode (a) rapidly grows. The observed initial growth rate of mode (a), $\gamma=0.085\omega_{pe}$, is in good agreement with the theoretical value. However, it soon saturates and is damped after the time $\omega_{pe}t\simeq 100$. Although mode (b) is almost stable in the initial state, it is destabilized at $\omega_{pe}t\simeq 100$. (In the weak current case with $v_{d0}=v_{Te}$,[19] the second harmonic H cyclotron wave was destabilized much later, at $\omega_{pe}t\simeq 600$.) The amplitude of mode (b) eventually becomes the same order of magnitude as that of the early stage of mode (a).

Figure 2 shows the frequency spectrum for mode (a) obtained from E_x and E_y for the period from $\omega_{pe}t=0$ to 1500. The peak is at $\omega\simeq 0.090\omega_{pe}$, which is in good agreement with the theoretical value $\omega\simeq 0.082\omega_{pe}$. The frequency spectrum for mode (b) is shown in Fig. 3. The highest peak is formed by the second harmonic H cyclotron wave. The observed frequency $\omega\simeq 2.52\Omega_H(=0.0504\omega_{pe})$ is higher than the theoretical value $\omega\simeq 2.02\Omega_H$ based on the initial conditions. As will be shown later, the increase of ω is caused by the electron temperature rise. In the weak current case, the observed frequency was in good agreement with the theory, and the rise of the electron temperature was only about 10%.

Figure 4 shows spectrum of H cyclotron waves as a function of the frequency and phase velocity $v_p(=\omega/k_\parallel)$. Fundamental, second, and third harmonic waves are plotted. The highest peak is at $\omega\sim 2.5\Omega_H$ and $v_p\simeq 3.0v_{Te}(=v_{d0})$. This is mode (b). The second harmonic wave with phase

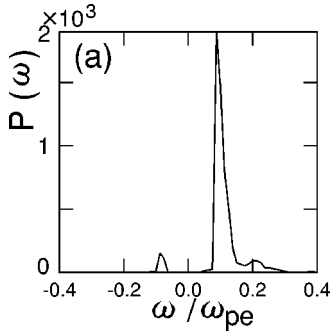

FIG. 2. Frequency spectrum for mode (a).

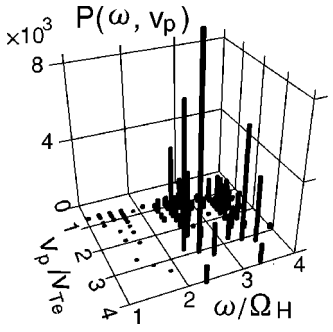

FIG. 4. Power spectrum of fundamental, second and third harmonic H cyclotron waves as a function of the frequency ω and phase velocity $\omega/k_\parallel$.

Downloaded 27 Oct 2006 to 133.6.32.11. Redistribution subject to AIP license or copyright, see http://pop.aip.org/pop/copyright.jsp

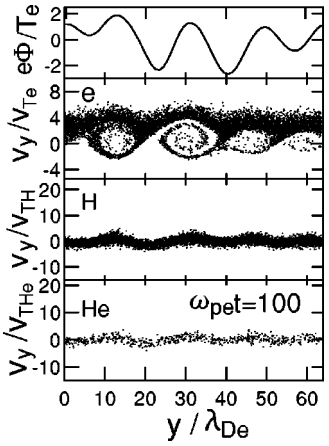

FIG. 5. Potential profile as a function of y (along the line $x/\lambda_{De}=1$) and phase space plots, (y,v_y) of electrons, H and He ions at $\omega_{pe}t=100$.

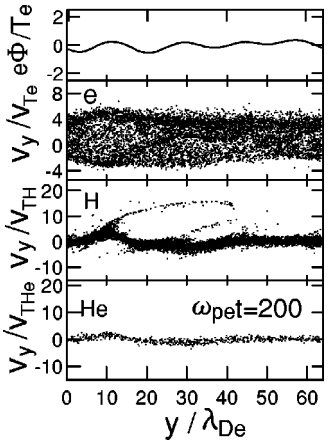

FIG. 6. Potential profile and phase space plots at $\omega_{pe}t=200$.

velocity equal to the initial electron drift speed v_{d0} eventually becomes dominant. This was also the case in the weak current case.[19]

B. Effect of Buneman waves

The Buneman waves produce electric potential larger than electron temperature. This potential traps some electrons, which saturates the waves.[28–30] Figure 5 shows a potential profile as a function of y (along the line $x/\lambda_{De}=1$) and phase space plots, (y,v_y) of electrons, H and He ions at $\omega_{pe}t=100$. Note that the magnetic field is in the y direction. In order to show the profile clearly, we plot the small region, $0\leqslant y/\lambda_{De}\leqslant 64$, although the total system length in the y direction is $L_y=1024$. The potential value is nearly constant in the x direction at this time. In the phase space, particles in the region, $0.5\leqslant x/\lambda_{De}\leqslant 1.5$ and $0\leqslant y/\lambda_{De}\leqslant 64$, are plotted. The electric potential ϕ is normalized to T_e/e where T_e is the initial electron temperature. The velocities of electrons, H and He ions are normalized to their thermal velocities, respectively.

Some electrons are trapped by the positive potential and form vortices in the phase space. The maximum amplitude of the wave is $2e\phi_0\simeq 4.2T_e$. Using this value, we can estimate the bounce frequency in this potential as $\omega_b\equiv\sqrt{e\phi_0 k^2/m_e}\simeq 0.091\omega_{pe}$. At around this time, ω_b becomes the same order of the initial growth rate $\gamma\simeq 0.088\omega_{pe}$ and the Buneman waves are saturated, as shown in Fig. 1.

After the Buneman waves are saturated, they are gradually damped because the wave energy is given to H ions. The energy transfer is due to the reflection by the potential. Figure 6 shows a potential profile and phase space plots (y,v_y) at $\omega_{pe}t=200$. We observe that there are some energetic H ions. They are reflected by the potential; some H ions are being reflected at $y\simeq 10$ around which the potential takes large positive values. After the reflection, those particles are accelerated by the negative potential and, at the bottom of it, they could have the maximum speed

$$v_{i\,\max}\simeq\frac{\omega}{k_\parallel}+2\sqrt{\frac{q_i\Phi_0}{m_i}}, \tag{3.1}$$

where $\omega/k_\parallel$ is the phase velocity of the Buneman wave and is much larger than the ion thermal speed. The reflected particles are not trapped by the potential, because the wave is gradually damped. (If the wave is not damped, the ion particles would be trapped by the potential well and the heating of H ions parallel to the magnetic field would not occur.) The reflected particles of H ions gain energies from the Buneman waves. On the other hand, He ions are not reflected by the potential and do not gain energies from the Buneman waves.

For the ion species i, the condition for the reflection by the potential can be written as

$$v\gtrsim v_{i\mathrm{ref}}, \tag{3.2}$$

with

$$v_{i\mathrm{ref}}=\frac{\omega}{k_\parallel}-2\sqrt{\frac{q_i\phi_0}{m_i}}. \tag{3.3}$$

As m_i increases, $v_{i\mathrm{ref}}$ increases and the thermal velocity v_{Ti} decreases. Hence, the fraction of reflected particles drastically decreases with m_i. If we substitute the observed value of ϕ at $\omega_{pe}t=100$ into Eq. (3.3), the critical speed of H ions is $1.2v_{TH}$. Some H ions satisfy Eq. (3.2). For He ions, the critical speed is much larger than thermal speed, $v_{i\mathrm{ref}}=5.1v_{THe}$. Hence, few He ions satisfy Eq. (3.2).

C. Electron velocity distribution function

We now discuss the change of the distribution function for electron parallel velocity, $f_e(v_y)$. Because of the electron trapping by the Buneman waves, $f_e(v_y)$ is drastically deformed and broadened. It finally has a plateau region with a width much wider than the initial thermal speed; in the weak current case, the width of the plateau region is about the same as the initial thermal speed.[19]

Figure 7 shows the evolution of $f_e(v_y)$. The vertical lines (a) and (b) represent parallel phase velocities of the Buneman wave ($\omega/k_\parallel=0.23v_{Te}$) and of the second harmonic H cyclotron wave ($\omega/k_\parallel=2.9v_{Te}$), respectively. Here, we calculate the values of their phase velocities using the values of the observed frequencies shown in Figs. 2 and 3. (The phase velocity of the Buneman wave is in good agreement

Downloaded 27 Oct 2006 to 133.6.32.11. Redistribution subject to AIP license or copyright, see http://pop.aip.org/pop/copyright.jsp

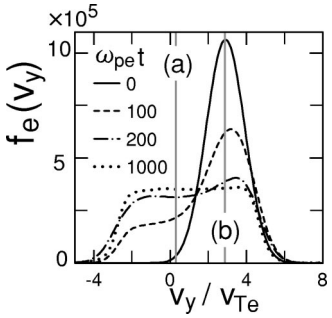

FIG. 7. Evolution of the distribution function for parallel electron velocity, $f_e(v_y)$. Vertical lines (a) and (b) represent parallel phase velocities of modes (a) and (b), respectively.

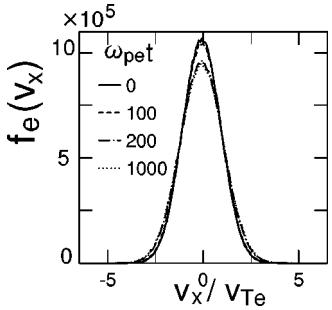

FIG. 8. Evolution of the distribution function for perpendicular electron velocity, $f_e(v_x)$.

with the theoretical value, $\omega/k_\parallel = 0.21$, while that of the H cyclotron wave is larger than the theoretical value, $\omega/k_\parallel = 2.2$.)

Initially, $f_e(v_y)$ is a shifted Maxwellian. However, the electron trapping due to the Buneman waves quickly broadens $f_e(v_y)$ by $\omega_{pe}t = 100$. Then, by $\omega_{pe}t = 200$, $f_e(v_y)$ has a large plateau region, $-2.8 \lesssim v_y/v_{Te} \lesssim 3.1$, with its center at line (a).

We can theoretically estimate the width of the plateau region made by the Buneman waves as[28]

$$|v_\parallel - \omega/k_\parallel| \lesssim 2(e\phi_0/m_e), \tag{3.4}$$

where ϕ_0 is the amplitude of the wave. The observed width is in good agreement with the theoretical value, $-2.6 \lesssim v_y/v_{Te} \lesssim 3.2$, where we have substituted the observed value of ϕ_0 at $\omega_{pe}t = 100$ into Eq. (3.4).

Let us focus on the region around line (b). Initially, the slope of $f_e(v_y)$ around line (b) is nearly zero. Therefore, mode (b) is marginal in the initial state. However, at $\omega_{pe}t = 100$ the slope becomes steep owing to the electron trapping by the Buneman waves. Then, the H cyclotron waves including mode(b) are destabilized. These waves, furthermore, make $f_e(v_y)$ flat around line (b). As a result, $f_e(v_y)$ eventually has a plateau region which is much larger than the initial thermal speed, $-3 \lesssim v_\parallel/v_{Te} \lesssim 4$.

After the time $\omega_{pe}t \simeq 100$, $f_e(v_\parallel)$ almost keeps its profile and growing modes are not observed. This indicates that, in this periodic system, the effect of circulation particles on the development of the instabilities would be small; before $\omega_{pe}t \simeq 1000$, there would be only small number of electrons which circulate the system with the length $L_y = 1024$.

Figure 8 shows the evolution of the perpendicular velocity distribution function, $f_e(v_x)$. The perpendicular function almost keeps its shape.

Figure 9 shows time variations of electron kinetic energy $T_{ej}(j = x,y)$, which is defined as

$$T_{ej} = \frac{\int d\boldsymbol{x} \int d\boldsymbol{v} f_e(\boldsymbol{v})(v_j(\boldsymbol{x}) - \langle v_j(\boldsymbol{x})\rangle)^2}{\int d\boldsymbol{x} \int d\boldsymbol{v} f_e(\boldsymbol{v})}, \tag{3.5}$$

where $\langle v_j(\boldsymbol{x})\rangle$ is the fluid velocity at the position $\boldsymbol{x}$

$$\langle v_j(\boldsymbol{x})\rangle = \frac{\int d\boldsymbol{v} f_e(\boldsymbol{v}) v_j(\boldsymbol{x})}{\int d\boldsymbol{v} f_e(\boldsymbol{v})}. \tag{3.6}$$

We calculate the fluid velocity at each time step. When $f_e(\boldsymbol{v})$ is Maxwellian, T_{ej} is the temperature. In Fig. 9, the solid and dashed lines represent T_{ex} and T_{ey}, respectively. They are normalized to their initial values. The parallel kinetic energy T_{ey} rapidly increases during the period $50 \lesssim \omega_{pe}t \lesssim 150$. This is caused by the electron trapping. After the time $\omega_{pe}t = 150$, T_{ey} becomes about 5.5 times as large as the initial value. As predicted by Eq. (2.14), the increase in T_{ey} enhances the frequency of H cyclotron waves; in Fig. 3, the observed frequency of mode (b) was higher than the theoretical value based on the initial conditions.

D. Heating of He ions

In this subsection, we discuss the energy transport among different particle species caused by the nonlinear evolution of the instabilities. It will be shown that He ions, which do not gain energies from Buneman waves, are eventually heated by H cyclotron waves.

We plot in Fig. 10 time variations of total kinetic energies of H and He ions. The solid and dashed lines represent parallel energy $K_\parallel$ and perpendicular energy $K_\perp$, respectively. They are normalized to their initial values. In H ions, the increase in $K_\parallel$ is greater than that in $K_\perp$. This is because the Buneman waves accelerate some H ions in the direction parallel to the magnetic field, as shown in Fig. 6. The increase in $K_\perp$ is mainly due to the collective motions forming H cyclotron waves. On the other hand, in He ions, $K_\perp$ eventually becomes larger than $K_\parallel$. In the early stage, $\omega_{pe}t \lesssim 150$, $K_\parallel$ and $K_\perp$ rapidly increase, as the Buneman waves grow. After $\omega_{pe}t \sim 150$, both of them decrease, as the Buneman waves are damped. At $\omega_{pe}t \sim 300$, $K_\perp$ starts to gradually increase, and, at $\omega_{pe}t = 1000$, it becomes about twice as large

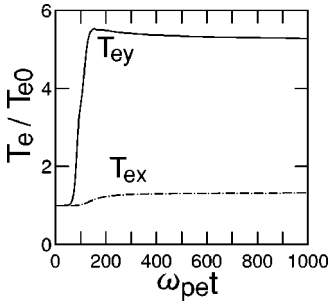

FIG. 9. Time variations of electron temperatures T_{ex} and T_{ey}.

Downloaded 27 Oct 2006 to 133.6.32.11. Redistribution subject to AIP license or copyright, see http://pop.aip.org/pop/copyright.jsp

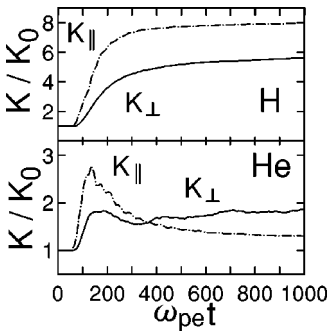

FIG. 10. Time variations of total kinetic energies of H and He ions.

as the initial value. The observed increase rate after $\omega_{pe}t=300$, $(dK_\perp/dt)/(K_{\perp 0}\omega_{pe})\simeq 4\times 10^{-4}$, is of the same order of the theoretical heating rate 10^{-4}. Here, we have substituted the observed values of ω and E_k of mode (b) by the simulation in Eq. (2.18). [If we use the theoretical value of ω based on the initial condition, the heating rate is much smaller. The frequency increase of mode (b), which was shown in Fig. 3, enhances the heating rate of He ions.]

Figure 11 shows distribution functions $f_{He}(v_\perp)$ for He ions at various times. The number of high energy particles increases with time. It is significant after the time $\omega_{pe}t=500$. The maximum $v_\perp$ exceeds $10v_{THe}$ at $\omega_{pe}t=1000$; in the weak current case,[19] it takes much longer time, $\omega_{pe}t\simeq 6000$, for $v_\perp$ to reach $10v_{THe}$. In the strong current case, the energy transfer to He ions occurs more rapidly than in the weak current case.

We show in Fig. 12 contour maps of the helium distribution function $f_{He}(v_\parallel,v_\perp)$ at four different times. The velocities are normalized to v_{THe}. The increase in $v_\perp$ of particles with $v_\parallel\simeq 0.75$ is noticeable. These particles satisfy the resonance condition, $\omega-5\Omega_{He}-k_\parallel v_\parallel\simeq 0$ with mode (b) ($\omega=2.52\Omega_H, k_\parallel\lambda_{De}=0.018$, and $k_\perp\lambda_{De}=0.17$). If the frequency of mode (b) were equal to the theoretical value, $\omega=2.02\Omega_H$, then there would be no resonance particles. The frequency increase of mode (b) plays an important role in the heating of He ions.

IV. SUMMARY

By means of a two-dimensional, electrostatic, particle simulation code, we have studied nonlinear evolution of instabilities driven by strong currents and associated energy transport among different particle species.

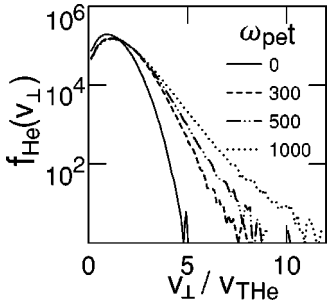

FIG. 11. Perpendicular helium velocity distribution, $f_{He}(v_\perp)$, at $\omega_{pe}t=0$, 300, 500, and 1000.

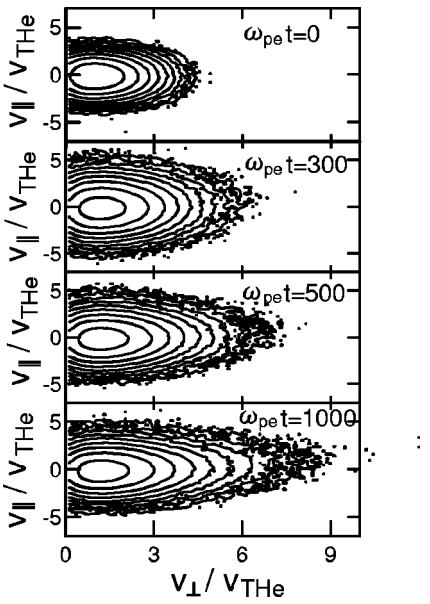

FIG. 12. Contour maps of $f_{He}(v_\parallel,v_\perp)$ at $\omega_{pe}t=0$, 300, 500, and 1000.

We considered a plasma consisting of H, He, and electrons with the density ratio $n_{He}/n_H=0.1$. The initial electron drift speed parallel to the uniform magnetic field was taken to be larger than the thermal speed, $v_{d0}=3v_{Te}$. According to the linear theory based on the initial conditions, the Buneman waves are the most unstable.

Certainly, simulations showed that the Buneman waves initially grow fastest and produce electric potential larger than the electron temperature. However, the Buneman waves quickly saturate owing to the electron trapping by the potential. They also reflect some H ions and accelerate them. On the other hand, He ions are not reflected and cannot gain energies from the Buneman waves. The electron trapping by the Buneman waves drastically changes the electron velocity distribution function $f_e(v_\parallel)$; thereby its width becomes about six times as large as the initial thermal speed. Then, H cyclotron waves are destabilized and grow to large amplitudes, although they are marginal in the initial state. Their frequencies are observed to be larger than the values predicted by the linear theory. This is caused by the rise of the electron temperature due to the Buneman waves. The H cyclotron waves can give energies to He ions through cyclotron resonances; in this process the frequency increase of the waves plays an important role. As a result, $f_e(v_\parallel)$ has a flat profile over a wide region, $-3\lesssim v_\parallel/v_{Te}\lesssim 4$, and He ions are heated perpendicularly to the magnetic field.

In the weak current case,[19] the H cyclotron waves, which are marginal in the initial state, are destabilized much later than in the strong current case. Also the frequencies of the H cyclotron waves are almost the same as those predicted by the linear theory, and the plateau region of $f_e(v_\parallel)$ was rather small, $0\lesssim v_\parallel/v_{Te}\lesssim 2$.

In this paper, we discussed the nonlinear development of electrostatic waves driven by the electron current and neglected the effects of electromagnetic waves. It is important to study those effects on the electron dynamics and on the

Downloaded 27 Oct 2006 to 133.6.32.11. Redistribution subject to AIP license or copyright, see http://pop.aip.org/pop/copyright.jsp

energy transfer to ions. In the future, we will study them using a electromagnetic simulation code.

ACKNOWLEDGMENT

This work was carried out by the joint research program of the Solar-Terrestrial Environment Laboratory, Nagoya University.

[1]O. A. Shaeffer and J. Zähringer, Phys. Rev. Lett. **8**, 389 (1962).
[2]J. D. Anglin, Astrophys. J. **198**, 733 (1975).
[3]D. V. Reames, Astrophys. J. **73**, 235 (1990).
[4]D. V. Reames, J. P. Meyer, and T. T. von Rosenvinge, Astrophys. J., Suppl. Ser. **90**, 649 (1994).
[5]G. J. Hurford, R. A. Mewaldt, E. C. Stone, and R. E. Vogt, Astrophys. J. Lett. **201**, L95 (1975).
[6]G. M. Mason, L. A. Fisk, D. Hovestadt, and G. Gloeckler, Astrophys. J. **239**, 1070 (1980).
[7]G. M. Mason, D. V. Reames, B. Klecker, D. Hovestadt, and T. T. von Rosenvinge, Astrophys. J. **303**, 849 (1986).
[8]E. G. Shelly, R. D. Sharp, and R. G. Johnson, Geophys. Res. Lett. **3**, 654 (1976).
[9]P. M. Kinter, J. Vago, S. Chesney, R. L. Arnoldy, K. A. Lynch, C. J. Pollock, and T. E. Moore, Phys. Rev. Lett. **68**, 2448 (1992).
[10]D. J. Knudsen, J. H. Clemmons, and J. Wahlund, J. Geophys. Res. **103**, 4171 (1998).
[11]M. André, P. Norqvist, L. Andersson, L. Eliasson, A. I. Eriksson, L. Blomberg, R. E. Erlandson, and J. Waldemark, J. Geophys. Res. **103**, 4199 (1998).
[12]P. J. Palmadesso, T. P. Coffey, S. L. Ossakow, and K. Papadopoulos, Geophys. Res. Lett. **1**, 105 (1974).
[13]L. A. Fisk, Astrophys. J. **224**, 1048 (1978).
[14]T. X. Zhang, M. Toida, and Y. Ohsawa, J. Phys. Soc. Jpn. **62**, 2545 (1993).
[15]T. X. Zhang and Y. Ohsawa, Sol. Phys. **158**, 115 (1995).
[16]S. Nakazawa, T. X. Zhang, and Y. Ohsawa, Sol. Phys. **166**, 159 (1996).
[17]M. Ashour-Abdalla and H. Okuda, J. Geophys. Res. **89**, 2235 (1984).
[18]M. Ashour-Abdalla, D. Schrier, and H. Okuda, J. Geophys. Res. **93**, 12826 (1988).
[19]M. Toida, T. Maeda, I. Shiiba, A. Sugishima, and Y. Ohsawa, Phys. Plasmas **7**, 4882 (2000).
[20]M. Toida and A. Sugishima, J. Phys. Soc. Jpn. **70**, 3285 (2001).
[21]O. Buneman, Phys. Rev. **115**, 503 (1959).
[22]B. D. Fried and R. W. Gould, Phys. Fluids **4**, 139 (1961).
[23]B. D. Fried and S. D. Conte, *The Plasma Dispersion Function* (Academic, New York, 1961).
[24]W. E. Drummond and M. N. Rosenbluth, Phys. Fluids **5**, 1507 (1962).
[25]J. M. Kindel and C. F. Kennel, J. Geophys. Res. **76**, 3055 (1971).
[26]J. M. Dawson, Rev. Mod. Phys. **55**, 403 (1983).
[27]A. B. Langdon, J. Comput. Phys. **6**, 247 (1970).
[28]T. O'Neil, Phys. Fluids **8**, 2255 (1965).
[29]O. Ishihara, A. Hirose, and A. B. Langdon, Phys. Rev. Lett. **44**, 1404 (1980).
[30]O. Ishihara and A. Hirose, Phys. Fluids **24**, 452 (1981).

Downloaded 27 Oct 2006 to 133.6.32.11. Redistribution subject to AIP license or copyright, see http://pop.aip.org/pop/copyright.jsp